PROGRESS IN PHOTOVOLTAICS: RESEARCH AND APPLICATIONS, VOL 1, 193–202 (1993)

Research

Emitter Design for High-efficiency Silicon Solar Cells. Part I: Terrestrial Cells

Jianhua Zhao, Aihua Wang and M. A. Green

Centre for Photovoltaic Devices and Systems, University of New South Wales, P.O. Box 1, Kensington 2033, Australia

Emitter diffusions for conventional high-efficiency silicon solar cells have commonly been designed to be very shallow to improve the short-wavelength response of the cells. This first part of a two-part paper has a substantial tutorial content and analyses the effect of the emitter design on cell performance with different cell surface passivation conditions. The analysis shows that shallow emitters are only necessary for cells with poor surface passivation. In contrast, high-efficiency cells with good surface passivation do not necessarily need shallow emitters. The application of these design insights into recent generations of high-efficiency passivated emitter solar cells is also discussed.

INTRODUCTION

One of the major stages in the history of silicon solar cell evolution was the development of violet cells with shallow junction emitters in the early 1970s.[1,2] These violet cells, with shallow junction emitters about 0.25 μm deep, significantly improved the blue (short wavelength) response of the cells and hence the efficiency. Since then, the idea of a shallow emitter has been widely accepted as important in high-efficiency silicon solar cell design. Another stage in the evolution of silicon cell design came in the early 1980s with improved surface and contact passivation with structures such as metal-insulator np-junction (MINP) cells and passivated emitter solar cells (PESC). The MINP cells and the first 20% PESC fabricated in the University of New South Wales before 1986 also had such shallow emitters.[3,4] These cells had emitter junctions depths of 0.2 μm, which is even shallower than the earlier violet cells. Many other research groups producing cell efficiencies close to 20% at the time also adopted shallow emitters, such as in the 19.8% cell made by Saitoh and co-workers at Hitachi[5] and the 19.5% cell made by Wood and colleagues at Oak Ridge National Laboratory.[6] The shallow emitter concept was so well accepted that many theoretical optimizations were made only for a 0.2 μm emitter junction depth.[7,8]

However, research at the University of New South Wales and elsewhere since 1986 has been directed towards the opposite: deep emitter silicon solar cells. This idea has also been addressed elsewhere, notably by Cuevas and Balbuena.[9] The first comprehensive theoretical analysis for the wide emitter depth range was published by King *et al.*[10] However, the main focus of the paper was rear point contact cells. Even though the result could be extended to more conventional cells with front emitter and metallization, the effect of front surface recombination and emitter junction depth was not emphasized. Subsequent publications[11,12] analysed a cell structure close to the passivated emitter and rear cell (PERC) developed at the University of New South Wales in 1988. These papers addressed the issue of efficiency limits for this particular cell structure. High surface recombination conditions, such as occur in commercial cells and space cells after radiation damage, were not addressed.

1062–7995/93/030193–10 $10.00

Received 22 March 1993
Revised 22 April 1993

Predating these latter studies, cells developed at the University with deep emitters include a 20.8% PESC (1988), a 22.3% PERC (1988) and a 23.3% passivated emitter and rear locally-diffused (PERL) cell (1990).[13–16] All these cells have deep emitters (deeper than 0.7 μm).

THEORETICAL ANALYSIS

Emitter surface passivation by a layer of thermally grown oxide in such high-efficiency cells significantly reduces recombination at the emitter surface. It not only improves the blue response of the cell, increasing the cell's short-circuit current density, but it also decreases the dark saturation current density, which improves the cell's open-circuit voltage.

Short-circuit current improvement

At the very short incident light wavelengths, the blue end of the solar spectrum, the light-generated minority carriers are all generated very close to the front surface of the cell owing to the high absorption coefficient at these wavelengths. The internal quantum efficiency $QE(\lambda)$ is determined entirely by the front emitter region[17] if a cell structure with a uniformly doped n-type emitter on a p-type substrate is assumed

$$QE(\lambda) = \frac{1 + S_p/[\alpha(\lambda)D_p]}{(S_p L_p/D_p)\sinh(W_N/L_p) + \cosh(W_N/L_p)} \tag{1}$$

where S_p is the surface recombination velocity for holes, L_p is the hole diffusion length, D_p is the hole diffusion coefficient, $\alpha(\lambda)$ is the photon absorption coefficient and W_N is the emitter junction depth. Because $\alpha(\lambda)$ is determined by the silicon material properties, only a large emitter carrier diffusion length L_p, a small emitter junction depth W_N and a low emitter surface recombination velocity S_p increase the short-wavelength quantum efficiency of the cells.

With the improvement of material technology, $W_N/L_p \ll 1$ is easily satisfied when the emitter is not extremely heavily doped. Hence, only a low S_p is required for a high short-wavelength response. It is also clear that a high short-wavelength response can be achieved when

$$S_p \ll D_p/L_p \tag{2}$$

For good cells, the critical S_p value is calculated to be around 10^5 cm s^{-1}. If S_p is much smaller than this value, the spectral response should be close to unity at the very short wavelength region. Also, it should be independent of the emitter junction depth.

For violet cells with shallow, heavily doped emitters and a high surface recombination velocity arising from the unpassivated emitter surfaces, the heavy doping in the emitter reduced D_p and τ_p and hence L_p and the critical S_p values. Hence, the short-wavelength response of the cell was improved for such unpassivated emitter surfaces by having the emitter thin. At the longer wavelengths where most of the carriers are generated in the base region, the effect of recombination at the front surface will be significantly reduced.

Open-circuit voltage improvement

On the other hand, the saturation current density J_0 also depends on the recombination inside the emitter (the base region) and at the emitter and rear surfaces. In the case of uniformly doped base and emitter regions where Boltzmann statistics suffice, J_0 is given as[18]

$$J_0 = \left(\frac{qD_n n_i^2}{L_n N_A} F_P + \frac{qD_p n_i^2}{L_p N_D} F_N\right) \tag{3}$$

where F_P and F_N are coefficients that incorporate the effect of surface recombination[18]

$$F_N = \frac{S_p \cosh(W_N/L_p) + D_p/L_p \sinh(W_N/L_p)}{D_p/L_p \cosh(W_N/L_p) + S_p \sinh(W_N/L_p)} \tag{4}$$

$$F_P = \frac{S_n \cosh(W_P/L_n) + D_n/L_n \sinh(W_P/L_n)}{D_n/L_n \cosh(W_P/L_n) + S_n \sinh(W_P/L_n)} \tag{5}$$

If the surface recombination velocities are very high. Equations (4) and (5) have the following forms

$$\left.\begin{aligned} F_N &= \coth(W_N/L_p) \\ F_P &= \coth(W_P/L_n) \end{aligned}\right\} \tag{6}$$

The coefficients F_N and F_P are then larger than unity, which will enlarge J_0.

If the surface recombination velocities are very low, Equations (4) and (5) have the following forms

$$\left.\begin{aligned} F_N &= \tanh(W_N/L_p) \\ F_P &= \tanh(W_P/L_n) \end{aligned}\right\} \tag{7}$$

The coefficients F_N and F_P are then smaller than unity, which will reduce J_0.

However, F_N and F_P will be at their lowest values only when

$$S_p \ll D_p/L_p \tag{8}$$

$$S_n \ll D_n/L_n \tag{9}$$

Equation (8) is the same limit as Equation (2) for the emitter short-circuit current limitation and Equation (9) is for the base; S_n has similar limiting values to those of S_p, about 10^5 cm s^{-1} for most cell conditions where $L_n \gg L_p$. If S_n and S_p are much smaller than these values, W_N is much smaller than L_n and W_P is much smaller than L_n, as for high-efficiency cells, Equation (3) becomes

$$J_0 = \left(\frac{qn_i^2}{N_A}\frac{W_P}{\tau_n} + \frac{qn_i^2}{N_D}\frac{W_N}{\tau_p}\right) \tag{10}$$

Hence, J_0 is proportional to $1/(N_D\tau_p)$ and $1/(N_A\tau_n)$. If the doping levels and the minority carrier lifetimes in the emitter and the base region are increased at the same time, J_0 is reduced. However, normally the minority carrier lifetime increases gradually for low doping levels below 10^{16} cm^{-3}, and then reduces very rapidly for higher doping levels heavier than 10^{18} cm^{-3} owing to the Auger recombination process.[2] In the cell emitter, the doping level is normally above 10^{18} cm^{-3}. Hence, when the emitter junction depth is increased, the surface doping level can be reduced to maintain the same saturation current density. This reduced emitter doping level will considerably increase the minority carrier lifetimes inside the cell emitter. This effect will result in a similar saturation current for a deep and lightly doped emitter as for a shallow and heavily doped emitter.

From the above analysis, a shallow emitter junction is essential when the emitter surface recombination velocity S_p is higher than the limiting value of around 10^5 cm s^{-1}. However, a shallow emitter junction is not necessary when S_p is much smaller than this value, such as when the cell surface is well passivated.

COMPUTER MODELLING RESULTS

The one-dimensional device simulation program, PC-1D,[19] is used to model the cell performance with different surface recombination velocities and different emitter profiles. Most of the important data used in the calculation are listed in Table I. The 0.5 Ω·cm p-type silicon substrate was used in the calculation because the best performances for PESC were achieved on such a substrate. The bulk carrier lifetime was chosen as 90 μs, which is also reasonable for PESC owing to the enhanced bulk carrier lifetime from

Table I. Data used to simulate the cell performance

Material	p-Si
Substrate resistivity	0.5 Ω·cm
Substrate thickness	280 μm
Front surface recombination velocity	Variable
Rear surface recombination velocity	Variable
Bulk carrier lifetime	90 μs
Intrinsic carrier concentration	1.01×10^{10} cm^{-3}
Auger coefficient for holes	9.9×10^{-32} cm^6 s^{-1}
Auger coefficient for electrons	2.8×10^{-31} cm^6 s^{-1}
Emitter surface doping concentration	Variable
Emitter junction depth	Variable
Emitter doping profile	Gaussian
Rear surface dopant	p-type
Rear junction depth	2 μm
Rear surface doping concentration	1×10^{19} cm^{-3}
Rear surface doping profile	Gaussian
Temperature	25°C

the aluminium gettering technique.[20] The subsequently developed PERC and PERL cells showed much higher bulk carrier lifetime and lower surface recombination velocities.

The calculated cell efficiency as a function of the emitter surface doping level and the emitter junction depth is shown in Figure 1 when the emitter and rear surface recombination velocity is 10^5 cm s^{-1}, which is the critical S_p value for the emitter surface. The recombination velocity at the rear surface has a much smaller effect on the cell performance than the recombination velocity at the front surface.

Thish high surface recombination corresponds to an unpassivated or poorly passivated cell. A large effect from S_p on the cell efficiency is expected. It is seen that the emitter junction depth is the most important parameter for the cell efficiency under this situation. Except for cells with very heavily doped surfaces, the cell efficiency decreases virtually linearly when the junction depth increases. This verifies perfectly the theory of violet cells. The highest calculated efficiency is similar to those that have been achieved by experimental shallow emitter devices.[3–6]

The calculated result is completely different if the emitter surface is well passivated with a lower surface

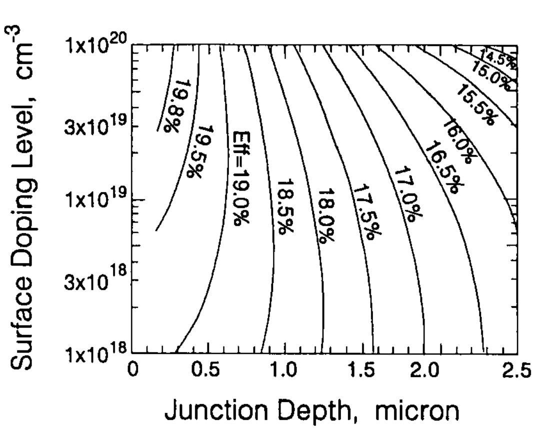

Figure 1. Calculated cell efficiency as a function of emitter surface doping levels and the emitter junction depth when the emitter and the rear surface recombination velocity is 10^5 cm s^{-1}. The junction depth is most important for the cell efficiency for this high surface recombination velocity

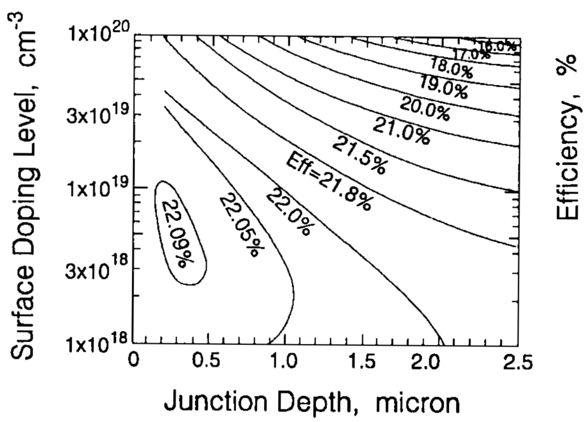

Figure 2. Calculated cell efficiency as a function of emitter surface doping level and the emitter junction depth when the emitter and the rear surface recombination velocity is 1000 cm s^{-1}. The junction depth is not critical for high cell efficiency for such a low surface recombination velocity

recombination velocity of 1000 cm s^{-1}. This result is shown in Figure 2. For this case, the maximum efficiency is on the left bottom corner of the figure, where the cells have a high surface doping level and a shallow junction, a medium surface doping level and a medium junction depth or a light surface doping level and a deep junction. High efficiency can be achieved for a wide range of emitter junction depths and surface doping levels in the area under the diagonal line in the figure. The emitter can be as deep as 2.5 μm as long as the surface doping level is low. However, if the surface doping level is high, the deep junction cells still have a much lower efficiency. Most of the improvement in Figure 2 compared to Figure 1 comes from an increased open-circuit voltage and an increased short-circuit current density owing to the reduced recombination at the surfaces. Hence, for high-efficiency cells it is very important to passivate cells surfaces in order to obtain recombination velocities much lower than the critical velocity.

A similar result to that in Figure 2 has been calculated for a surface recombination that is much smaller than 1000 cm s^{-1}, because any lower surface recombination velocity will not affect the total recombination when bulk recombination is dominant.

The emitter surface sheet resistance is also determined by the emitter surface doping level and the emitter junction depth, as is shown in Figure 3. Two interesting results can be deduced from the figure.

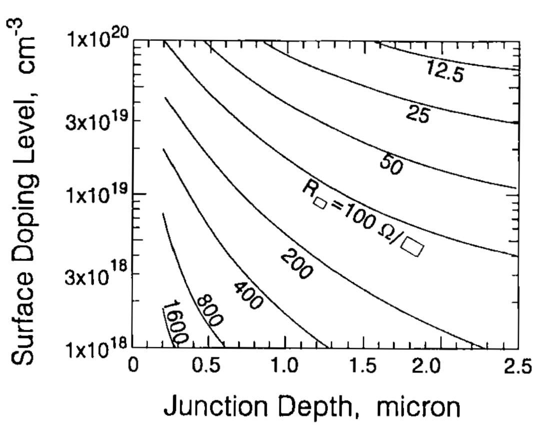

Figure 3. Emitter sheet resistance as a function of emitter surface doping level and the emitter junction depth. The curves are similar to those in Figure 2 at the right upper corner of the figure

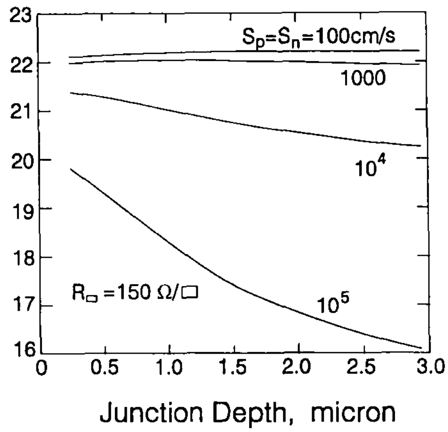

Figure 4. Calculated cell efficiency as a function of the emitter junction depth and surface recombination velocities; S_p and S_n are the surface recombination velocities at the front and the rear surfaces. A shallow junction only produces benefits when the surface recombination velocity is higher than 1000 cm s^{-1}

The first is that the equal sheet resistance lines are very close to the equal efficiency lines in the area at the right upper half in Figure 2. Hence, the emitter sheet resistance is most important in determining the efficiency for cells with well-passivated surfaces. The second is that the area with a sheet resistance higher than 150 Ω/□ is the optimum area for the cell efficiency.

This sheet resistance value of 150 Ω/□ is also the optimum experimental value for PESC, PERC and PERL cells. Hence, the following calculations from Figure 4 to Figure 6 used only the optimum sheet resistance of 150 Ω/□.

Figure 4 shows the relation between the cell efficiency and the emitter junction depth. The emitter sheet resistance is fixed at the optimized value of 150 Ω/□ from earlier analysis. The same high-efficiency limit will be achieved if the surface recombination velocity is lower than 1000 cm s^{-1}. The efficiency is independent of the emitter junction depth for these low surface recombination velocities. However, when the surface recombination velocity is high, shallow emitter cells perform much better than the deep emitter cells.

The cell efficiency reduction comes mostly from the reduction of the short-circuit current density for the high surface recombination cases with 150 Ω/□ emitter sheet resistance. The cell internal quantum efficiency was also calculated to determine the origin of the current loss. Figure 5 shows the calculated internal quantum efficiency for a shallow junction cell, whereas Figure 6 shows the calculated internal quantum efficiency for a deep junction cell.

It is interesting to compare Figure 5 with Figure 6. The violet cell with a shallow emitter 0.25 μm deep and a high surface recombination velocity of 10^5 cm s^{-1}, as shown in Figure 5, does have a slightly reduced short-wavelength response below a 0.5-μm wavelength. The response increases to unity at longer wavelength when most photons are generated underneath the emitter junction, as predicted earlier in the last section. It is also true that the 2-μm deep junction cell with good surface passivation and low surface recombination velocity below 10^3 cm s^{-1}, as shown in Figure 6, has unity response even to the very short wavelength band. However, once the surface recombination velocity is increased to over 1000 cm s^{-1}, the cell will have considerable loss in this short-wavelength range.

In fact, the surface recombination velocity also increases with the surface doping levels owing to the increased stresses in the lattice and dislocations caused by the diffusion.[21] The surface recombination velocity also depends on the surface passivation processing conditions. A surface with a layer of silicon dioxide grown in 1,1,1-trichloroethane (TCA) has a much better surface passivation than without this layer. It is also better than with the normal wet oxidation method with oxide grown in steam. Work by

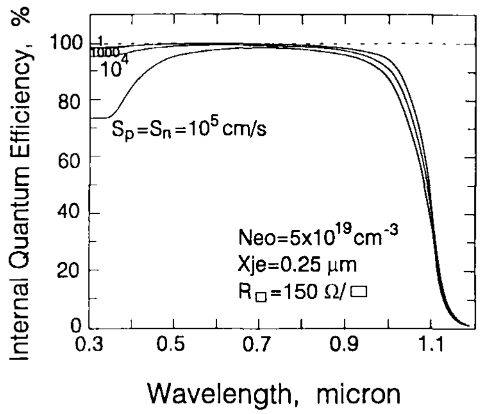

Figure 5. Calculated internal quantum efficiency curves as a function of the surface recombination velocity for 0.25-μm shallow emitter cells. Neo and Xje are the emitter surface doping level and the emitter junction depth, respectively. A high surface recombination velocity causes only a small quantum efficiency drop at the very short wavelength range

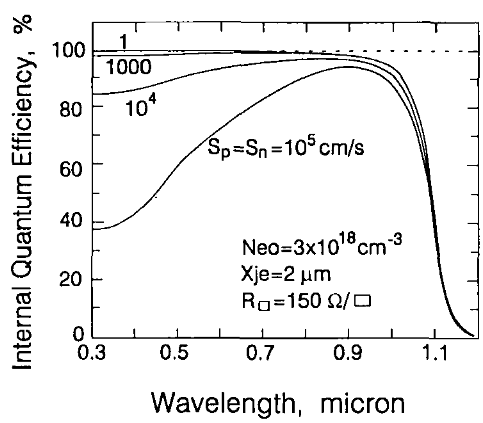

Figure 6. Calculated internal quantum efficiency curves as a function of the surface recombination velocity for 2-μm deep emitter cells. Neo and Xje are the emitter surface doping level and the emitter junction depth, respectively. A high surface recombination velocity causes a large quantum efficiency drop at the short and the medium wavelength range

Swanson and co-workers has shown that silicon dioxide grown in TCA has a surface recombination velocity of 1000 cm s^{-1} on a phosphorus-diffused surface with a surface doping level of 4×10^{19} cm^{-3}.[10] The surface recombination velocity is lower than this value for lower surface doping levels.

EMITTER PROFILES FOR PESC, PERC AND PERL CELLS

As discussed earlier, the early PESC followed the trend of shallow emitter design.[4] They had emitter junctions about 0.2 μm deep. However, it was subsequently found that deep emitter PESC, with the thin passivation oxide grown at higher temperature, showed a considerably improved performance.

The improved PESC and the subsequently developed PERC and PERL cells are fabricated with an

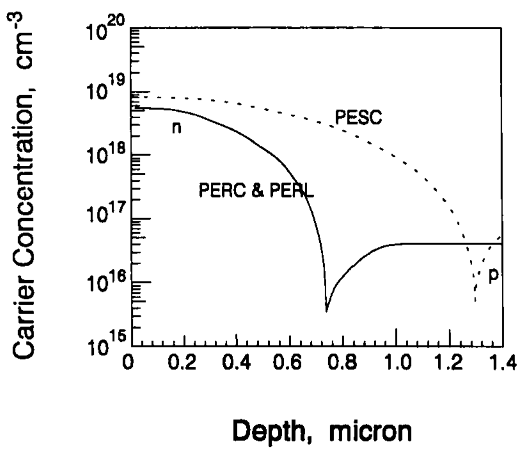

Figure 7. Emitter doping profiles for high efficiency PESC, PERC and PERL cells

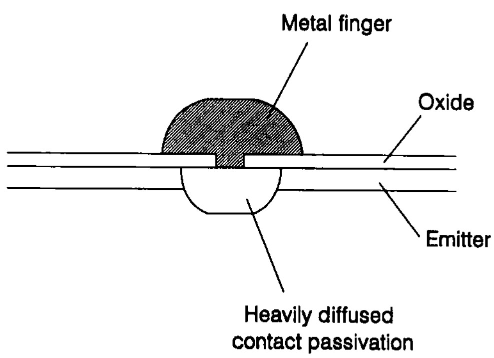

Figure 8. The metal contact areas of the high efficiency PERC and PERL cells are passivated by heavily diffused areas

emitter depth of 0.7–1.5 μm and a surface sheet resistance of about 150 Ω/□. Figure 7 shows typical emitter doping profiles for these cells. The surface doping levels for these cells are below 1×10^{19} cm^{-3}. Most PERC and PERL cells have very lightly diffused emitters. However, some of the most recent PERL cells with a heavier emitter diffusion of about 150 Ω/□ sheet resistance show the same good performance. Actually, experimental attention was paid to improving the surface passivation but little was paid to the emitter junction depth. This is because, for PESC, PERC and PERL cells with good emitter surface passivation, the emitter junction depth experimentally has little effect on the cell efficiency, as predicted by the previous theory.

The PERC and PERL cells demonstrated higher performance than PESC cells owing to the low surface recombination velocities and the higher bulk minority carrier lifetimes generated by the TCA-based processing.[14] Recombination at the front metal contact under the fingers becomes important for PERC and PERL cells owing to the significantly improved bulk carrier lifetime and the emitter surface passivation by the TCA-based processing. Hence, these areas in the PERC and PERL cells are further passivated by more heavily doped diffused areas with a sheet resistance below 10 Ω/□, as shown in Figure 8. This two-step diffusion procedure also allows separate optimization for the emitter surface passivation and the front metal contact passivation areas.

CONCLUSION

Both theoretical analysis and experiments show that high-efficiency silicon cells with good surface passivation do not necessarily need shallow emitters. On the contrary, conventional cells with poor surface passivation perform best with shallow emitters. Hence, the optimum emitter profile is actually determined by the surface passivation conditions. All recent high-efficiency PESC, PERC and PERL cells have deep emitters of over 0.7 μm depth. Separate, heavily diffused areas are also incorporated to passivate further the front metal finger contact areas for PERC and PERL cells.

Acknowledgements
This work was supported by the Australian Research Council and Sandia National Laboratories. The Centre for Photovoltaic Devices and Systems is supported by the Australian Research Council and Pacific Power.

REFERENCES

1. J. Lindmayer and J. Allison, 'The violet cell: an improved silicon solar cell', *COMSAT Tech. Rev.*, **3**, 1–22 (1973).
2. M. A. Green, *High Efficiency Solar Cells*, Trans Tech Publications, Switzerland, 1987.
3. M. A. Green, A. W. Blakers, J. Shi, E. M. Keller and S. R. Wenham, 'High efficiency silicon solar cells', *IEEE Trans. Electron. Dev.*, **ED-31**, 679–683 (1983).
4. A. W. Blakers and M. A. Green, '20% Efficiency silicon solar cells', *Appl. Phys. Lett.*, **48**, 215–217 (1986).
5. T. Saitoh, 'Recent technological advances in crystalline silicon solar cells in Japan', *Proceedings of the 9th European Communities Photovoltaic Solar Energy Conference*, Freiburg, pp. 362–365, September (Kluwer, Dordrecht) 1989.
6. R. F. Wood, R. D. Westbrook and G. E. Jellison, Jr., 'High-efficiency intrinsically and extrinsically passivated laser-processed silicon solar cells', *Conference Record of the 19th IEEE Photovoltaic Specialists Conference*, New Orleans, pp. 519–524, May 1987.
7. A. Morales-Acevedo, 'On the optimum surface dopant concentration in high efficiency solar cells', *Conference Record of the 18th IEEE Photovoltaic Specialists Conference*, Las Vegas, pp. 1750–1751, October 1985.
8. E. I. H. Lin, 'Sensitivity analysis of low bulk resistivity solar cells', *Conference Record of the 18th IEEE Photovoltaic Specialists Conference*, Las Vegas, pp. 715–719, October 1985.
9. A. Cuevas and M. Balbuena, 'Thick-emitter silicon solar cells', *Conference Record of the 20th IEEE Photovoltaic Specialists Conference*, Las Vegas, pp. 429–434, September 1988.
10. R. R. King, R. A. Sinton and R. M. Swanson, 'Studies of diffused phosphorus emitters: saturation current, surface recombination velocity, and quantum efficiency', *IEEE Trans. Electron Dev.*, **ED-37**, 365–371 (1990).
11. J. Knobloch, A. Aberle, W. Warta and B. Voss, *Proceedings of the 5th Photovoltaic Solar Energy Conference, Kyoto*, (Showado Insatsu K.K., Japan), November 1990.
12. A. Aberle, W. Warta, J. Knobloch and B. Voss, *Conference Record of the 21st IEEE Photovoltaic Specialists Conference, Kissimmee*, Orlando, May 1990.
13. M. A. Green, J. Zhao, A. Wang, C. M. Chong, S. Narayanan, A. W. Blakers and S. R. Wenham, 'Improvements in silicon solar cell efficiency', *The 8th European Communities Photovoltaic Solar Energy Conference, Florence, Italy*, May, pp. 164–167, 1988 (Kluwer Academic Publishers, Dordrecht).
14. A. W. Blakers, J. Zhao, A. Wang, A. M. Milne, X. Dai and M. A. Green, '23% Efficient silicon solar cell', *The 9th European Communities Photovoltaic Solar Energy Conference, Freiburg*, September, pp. 328–329, 1989 (Kluwer Academic Publishers, Dordrecht).
15. A. Wang, J. Zhao and M. A. Green, '24% Efficient silicon solar cells', *Appl. Phys. Lett.*, **57**, 602–604 (1990).
16. M. A. Green, 'Recent advances in silicon solar cell performance', *Proceedings of the 10th European Communities Photovoltaic Solar Energy Conference, Lisbon*, April, pp. 250–253, 1991 (Kluwer Academic Publishers, Dordrecht).
17. S. M. Sze, *Physics of Semiconductor Devices*, 2nd Edn., Wiley, New York, 1981.
18. M. A. Green, *Solar Cells—Operating Principles, Technology and System Applications*, Prentice-Hall, New Jersey, 1982.

19. D. T. Rover, P. A. Basore and G. M. Thorson, 'Solar cell modelling on personal computers', *Conference Record of the 18th IEEE Photovoltaic Specialists Conference*, Las Vegas, pp. 703–709, October 1985.
20. S. Narayanan, S. R. Wenham and M. A. Green, 'High efficiency polycrystalline silicon siolar cells using phosphorus pretreatment', *Appl. Phys. Lett.*, **48**, 873–875 (1986).
21. T. H. Yeh and M. L. Joshi, 'Strain compensation in silicon by diffused impurities', *J. Electrochem. Soc.*, **116**, 73–77 (1969).